Inhibiting Spasticity by Blocking Nerve Signal Conduction in Rats With Spinal Cord Transection

Jianjun Zhang, Guangwei Mao, Yunhua Feng, Bin Zhang, Baiyun Liu, Xiaoying Lü, and Zhigong Wang, *Senior Member, IEEE*

***Abstract*— Spasticity is a common motor disorder following a variety of upper motor neuron lesions that seriously affects the quality of patient's life. We aimed to evaluate whether muscle spasms can be suppressed by blocking nerve signal conduction. A rat model of lower limb spasm was prepared and the conduction of pathological nerve signals were blocked to study the inhibitory effect of nerve signal block on muscle spasm. The experimental results showed that 4 weeks after the 9th segment of the rat's thoracic spinal cord was completely transacted, the *H*/*M*-ratio of the lower limbs increased, and rate-dependent depression was weakened. When the rat model was stimulated by external forces, the electromyography (EMG) signals of the spastic gastrocnemius muscles continued to erupt. After blocking the conduction of nerve signals in the rat sciatic nerve, the spastic EMG signal of the gastrocnemius muscle disappeared. The effective blocking time and blocking efficiency increased with increasing blocking signal amplitude, and the maximum blocking efficiency reached 73%. The experimental results of this study proved the feasibility of inhibiting lower limb spasticity by blocking nerve signal conduction.**

***Index Terms*— Spasm inhibition, nerve signal block, spastic rat model, spike trapping.**

I. Introduction

SPASTICITY is common in a variety of central nervous system diseases, such as stroke, spinal cord injury, cerebral palsy, and multiple sclerosis [1]. Approximately 20% to 40% of stroke patients and 50% to 60% of spinal cord injury patients experience spasticity [2], [3]. Muscle spasms can interfere with the patient's spontaneous movement control, seriously affect the patient's quality of life, and places a huge burden on the patient's family and society. Thus, it has become an urgent clinical problem to be solved and a hot research topic [4]–[6].

The study of spasticity relies on appropriate animal models and measurement methods that can sensitively detect the differences of spasticity in model animals. In 1992, Ritz *et al.* injured a cat's lower sacral spinal cord, causing spasm of its tail muscles [7]. In 1999, Bennett *et al.* established a commonly used rat tail muscle spasm animal model by damaging the S2 spinal cord of rats [8]. This spasm model usually does not affect the intestines, bladder or lower limbs of the animal, causes little damage, and has the advantages of simple care and a high survival rate. However, the tails of animals are very different from the lower limbs of humans, and the clinical features of spasticity are rarely reflected in the tails of spasmodic animal. In 1997, Kanellopoulos *et al.* used balloon embolization to block blood flow at the aortic level and prepared spinal cord injury models with different degrees of injury [9]. In 2002, Sufianova *et al.* established a spinal cord ischemic injury rat model by occluding the abdominal aorta and its branches to cause transient lumbar spinal cord ischemia [10]. This ischemic spinal cord injury model has been proven to be able to simulate lower limb spasticity after human spinal cord injury. However, the model preparation is complicated, requires very skilled surgical techniques, and extensive nursing care and is associated with a high mortality. In 1911, Allen *et al.* designed a spinal cord dorsal blow model, using hammers with different weights to fall vertically along a set of tubes from different heights to hit the dorsal spinal cord, causing varying degrees of injury. Other researchers continued to improve that method and created a spinal cord injury spastic model that is more consistent with clinical spinal cord injury [11]. That method is simple to apply, but the degree of damage is not easy to control, and the incidence of spasms is low. In 2015, Jose *et al.* prepared an animal model of lower extremity spasms by completely severing the thoracic T9 spinal cord segments of the rat [12]. This model is stable and reliable, and the procedure is relatively easy. In this paper, the same method was used to prepare an animal model of spasm.

In addition to the preparation of suitable animal spasm models, quantitatively evaluating spasticity in animal models is also crucial. After the thoracic spinal cord is injured, the dis-inhibition of the motor neuron from descending pathways and changes in per-synaptic inhibition lead to changes in

Manuscript received May 17, 2021; revised July 23, 2021 and August 25, 2021; accepted October 19, 2021. Date of publication November 1, 2021; date of current version November 17, 2021. This work was supported in part by the National Natural Science Foundation of China under Grant 61534003, Grant 62004036, and Grant 61874024; and in part by the Science and Technology Pillar Program of Jiangsu Province under Grant BE2016738. *(Jianjun Zhang and Guangwei Mao contributed equally to this work.) (Corresponding authors: Xiaoying Lü; Zhigong Wang; Baiyun Liu.)*

Jianjun Zhang, Guangwei Mao, Yunhua Feng, and Xiaoying Lü are with the State Key Laboratory of Bioelectronics, Southeast University, Nanjing 210009, China (e-mail: luxy@seu.edu.cn).

Bin Zhang and Baiyun Liu are with the Beijing Tiantan Hospital, Beijing 100070, China (e-mail: liubaiyun1212@163.com).

Zhigong Wang is with the Institute of RF- & OE-ICs, Southeast University, Nanjing 210009, China (e-mail: zgwang@seu.edu.cn).

Digital Object Identifier 10.1109/TNSRE.2021.3124530

the activity of the interneurons and motor neurons in the segment and changes in the corresponding electrophysiological activity. Among them, the H/M-ratio and the rate-dependent-depression (RDD) of the Hoffmann (H) reflex are often used as indicators to evaluate the degree of spasm. When a weak electrical stimulus is applied to the nerve, only the sensory neuron is activated first. After sensory nerve signals are transmitted to the spinal cord through the afferent nerves, the corresponding anterior horn of the spinal cord is excited, and the corresponding nerve excitement is transmitted through the efferent nerves. The EMG signal recorded at this time is H-wave. When the stimulation intensity is sufficient to activate the motor neuron, another pulse waveform appears before the recorded H-wave, which is the M-wave. As the stimulus intensity increases, the H-wave amplitude first increases, then decreases, and finally disappears. The M-wave will increase to the maximum and remain unchanged. In addition, researchers also directly record electromyography (EMG) activity of the target muscle to reflect the degree of spasticity. Shi G X *et al.* found that in spastic rats, as the activity of the spinal motor neurons increases, the H-reflex amplitude increase, but the M-wave amplitude will not change, resulting in an increase in the $H_{\max}/M_{\max}$-ratio [13]. Lee *et al.* reported that by gradually increasing the stimulation frequency, the amplitude of the H reflex in normal rat muscles was inhibited. In spastic rat, the amplitude of the H-reflex was not significantly reduced under high-frequency stimulation [14].

Current clinical treatments for spasticity are focused on drug therapy, surgery and physical therapy. Drug therapy usually involves the injection of botulinum toxin and oral baclofen. Although they are widely used, there is insufficient evidence to ensure that cramps can be reduced through drug therapy, and there are possible side effects [15]–[17]. For tonic spasticity that seriously affects the posture of the patient's lower limbs, clinically, the dorsal root nerve of the spinal cord is selectively cut for treatment, but the operation is irreversible and will cause partial loss of sensation.

In the past two decades, many physical therapy methods have been applied to rehabilitation exercises for patients with spinal cord injury, but they are time-consuming and costly [18], [19]. Recently, functional electrical stimulation has been applied to the clinical treatment of patients with spinal cord injury, and it is considered to have a beneficial effect on the suppression of spasticity. Related neuromuscular electrical stimulation methods have also received attention.

High-frequency (HF) alternating electrical nerve stimulation techniques with the ability to reversibly block nerve signal conduction have been extensively studied [20], [21]. From the 1960s, Tanner and others used HF alternating currents to stimulate nerves and block the conduction of nerve signals. Many researchers have studied the related problems that affect the results of HF blocking through computer simulations or acute and long-term animal experiments, and there have been reports of its application in clinical analgesia [22]–[25]. However, there is a shortcoming to be resolved. In the initial stage of applying an HF alternating current, blocking current would cause nerve excitement. Although researchers have used electrode optimization [26], waveform optimization [27]–[30], and electrical stimulation combined with freezing and other methods [31] to reduce the impact of the initial response, they cannot completely make up for the deficiency. Even if the researchers used the DC+HF block method to eliminate the initial response, the DC block requires a slow rising period and cannot instantly block nerve signal conduction [27].

In previous studies by our research group, we proposed a blocking method that can instantly block nerve signal conduction without causing nerve excitement—the spike trapping nerve block (STNB) [32]. The ultimate aim of the STNB is to block the pathological neural signals at the appropriate time and position after the detecting electrode located at the proximal end detects the non-autonomous pathological neural signals. For this end, we explored the suitable blocking signal waveform parameters and electrode configuration that affect its blocking effect [32], [33]. The thresholds for the transverse electrode configuration were lower than that of electrodes placed longitudinally along the nerve, however, it required that the anode-nerve contact area must be larger than the cathode-nerve contact area, and an optimum anode width was found to be 5 mm.

This paper uses the blocking waveform parameters and transverse electrode configuration obtained in the previous experiments to explore the feasibility of suppressing lower extremity spasticity with the STNB blocking signals on the spastic rat model with 9th thoracic spinal cord complete transection. We only evaluated the possibility of inhibiting spasticity by blocking nerve signal conduction, and did not achieve true STNB. In other words, what we blocked is the conduction of all nerve signals, and did not recognize spastic nerve signals.

II. Materials and Methods

A. Modeling of Spastic Rat

All animal experimental procedures in this study conformed to the guidelines for the care and use of laboratory animals at Southeast University (20190720001). The experiments used adult female Sprague-Dawley rats (200-300 grams, provided by the Zhejiang Laboratory Animal Centre, license number: SCXK (Zhejiang) 2019-0002).

Before the operation, the rat was placed in an anesthesia box and was quickly anesthetized with 5% isoflurane (RWD, Shenzhen, China). Then, the rat was fixed on a rat board and placed on a breathing mask. During the operation, 2%∼3% isoflurane was used to maintain anesthesia according to its breathing rate and paw pinch reflex. The rat's back hair was shaved and the skin was washed and disinfected with 75% alcohol and iodophor. After cutting the back skin, under the operating microscope, the paravertebral muscles around the T8 vertebral body were removed. We used rongeur to clamp the spinous process and slightly lift it up. The laminectomy of the T8 vertebral body was carefully completed with ophthalmic scissor and the T9 spinal cord was perfectly exposed. The spinal cord was hooked and lifted up with a dural hook. Ophthalmic scissor was used to cut off the spinal cord about 2-mm wide, and the remaining tissue was removed along the vertebral wall with beak tweezer. A hemostatic sponge was

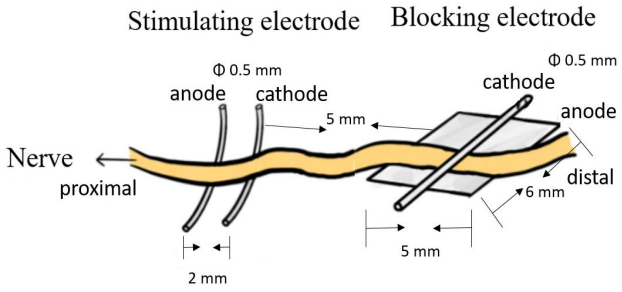

Fig. 1. Schematic diagram of the relative position of the electrodes and nerves.

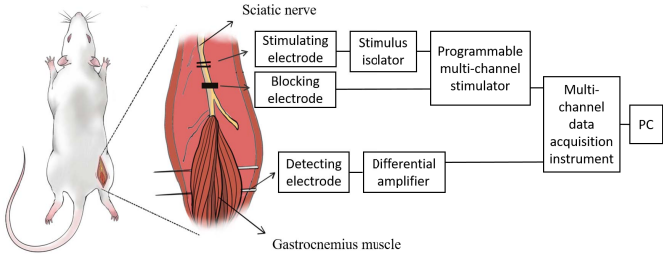

Fig. 2. Schematic diagram of the experimental instrument connection.

inserted into the incision, and the muscle and skin were sutured with absorbable suture. After the operation was completed, the rats were awakened in an incubator and cared for individually. For 4∼7 days after the operation, the rats were given oral amoxicillin (Maclin, Shanghai, China) at 10 mg per day to prevent wound infection. The rats were maintained for 4 weeks. The light-dark cycle was controlled at 12:12 hours, and the environmental temperature was controlled at approximately 23 °C. During this period, the rats could freely obtain food and water and were allowed to urinate artificially 3 times a day.

B. Operation Process and Electrical Equipment Connection Before the Experiment

Before the experiment, the animals in the study had normal appetite, relatively stable mental state, and good physical health. The rats were anesthetized with isoflurane as described above. We selected a hind leg with full muscles and intact skin and smooth hair (as a result of lower limb paralysis, muscle atrophy and skin ulceration of long-term lateral lying side leg was appeared, the other side leg was selected), shaved off the hairs, made an incision along the outside of the thigh with a scalpel, peeled off the quadriceps, and completely exposed the whole sciatic nerve from the spine to its distal branch. The stimulation electrode was placed at the proximal end of the sciatic nerve, and the blocking electrode was placed at the distal end of the sciatic nerve, with a distance of 5 mm between two electrodes. As shown in Fig. 1, the stimulation electrode was consisted of a pair of platinum wires with a diameter of 0.5 mm, which are placed on the side of the nerve along the longitudinal direction. The anode of the stimulating electrode is located at the proximal end of the nerve, and the cathode is located at the distal end of the nerve. The distance between anode and cathode is 2 mm. The blocking electrode was an asymmetric bipolar electrode. The anode is a platinum sheet with a width of 5 mm and a length of 6 mm, and the cathode is a platinum wire with a diameter of 0.5 mm. The electrodes were placed on both sides of the nerve in the lateral direction.

As shown in Fig. 2, the stimulation electrode was connected to a programmable multichannel stimulator (Master9, Israel AMPI) through a stimulation isolator (ISO-Flex, Israel AMPI). The blocking electrode was directly connected to the programmable multichannel stimulator (Master9, AMPI, Israel). The stimulus signal is a current-controlled one, and the blocking signal is a voltage-controlled one. The detecting electrode was inserted into the gastrocnemius muscle with a sewing needle and tied at one end for fixation. The detecting electrode is made of stainless steel wire with an insulating layer on the outer surface (Kedou, Jiangsu, China), and the insulating layer of approximately 1 cm is removed at both ends. The detecting electrode was in contact with the gastrocnemius muscle and the biological signal amplifier (differential AC amplifier model 1700, American AM System). The magnification of the amplifier is 1000, and the passband is 10∼5 kHz. The output signals of the bio-signal amplifier, the stimulation signal and the blocking signal are transferred to a 16-channel data acquisition system (Power Lab, AD Instruments, Australia), and the sampling rate is 10 kHz/s.

The multichannel data acquisition system transmits the data to the LabChart software on the PC for real-time display, processing and storage of the data.

C. Measurement of Hoffman Reflex and Rate-Dependent Depression

After completing the operation and the instrument connection, we adjusted the multichannel programmable stimulator and the stimulation isolator to output a negative pulse stimulating sequence with increasing amplitude (150∼300 μA, 10 μA increments, 0.1 Hz, 200 μs). The stimulation signals were applied to the sciatic nerve through the stimulation electrodes. The stimulation signals and the corresponding gastrocnemius EMG signal were recorded to determine the amplitude of the M-wave and H-wave and to calculate the ratio of $H_{\max}/M_{\max}$. The stimulation pulse of each current intensity was applied 8 times, and the average value was taken as the amplitude of H-wave and M-wave of a single rat. To measure the RDD of the rats, 20 negative stimulating pulses with a frequency of 0.1 Hz were applied to the rat's sciatic nerve. Then, changing the frequency to 0.5, 1, 5, and 10 Hz, respectively, the amplitude of the rat H-reflex was recorded and compared with different frequencies. We randomly select 8 H-wave and take the average value as the RDD H reflection value of a single rat.

D. Induction and Measurement of Muscle Cramps

The T9 spinal cord transection rat that was completed the operation and awake was fixed in a PVC tube to restrict its movement. The EMG signal of the gastrocnemius muscle was recorded for 2 minutes. A pressure gauge was used to press

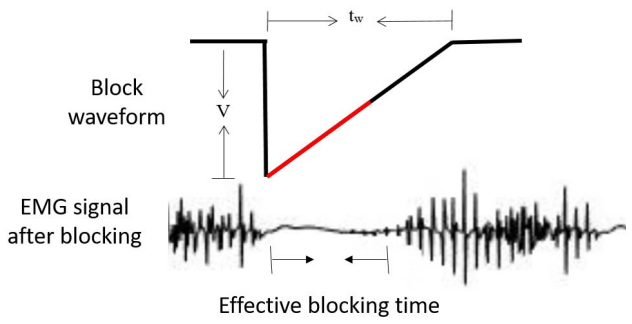

Fig. 3. Schematic diagram of the blocking signal (the red line indicates the effective blocking time, not a fixed value).

the rat's Achilles tendon. The pressure was kept at 1∼2 N, pressing for 3 s and stopping for 3 s each time, pressing 10 times, and the gastrocnemius EMG signal was recorded before and after the pressure stimulation.

E. Minimum Pulse Width Measurement Under Different Blocking Signal Amplitude

Simultaneous application of the stimulation signal and the blocking signal were given to the sciatic nerve through the stimulation electrode and the blocking electrode. As shown in Fig. 3, the waveform consists of an instantaneously decreasing voltage V, which then increased linearly to zero with time t_w. The stimulation signal is a single negative pulse with an amplitude of 1 V and a pulse width of 200 μs. The minimum pulse width of the blocking signal that can block nerve signal conduction without causing nerve excitement is defined as the minimum pulse width. The initial parameters of the blocking signal are set to 3 V in amplitude and 300 ms in pulse width. Keeping the amplitude unchanged, first we gradually reduced the pulse width to 100 ms in 100 ms steps. If muscle contraction occurs during this period, we started from the pulse width when the muscle contraction occurs, and gradually increased the pulse width in 10 ms steps until the nerve signal was completely blocked. The pulse width at this time is the minimum pulse width. If the pulse width is reduced to 100 ms and the nerve signal transmission can still be completely blocked, then the nerve signal transmission can be gradually reduced in steps of 10 ms, and the previous pulse width is the minimum pulse width. After completing the above process, the blocking signal amplitude was set to 3.5, 4, 4.5, 5, 5.5, and 6 V in turn, and the experimental process above was repeated.

F. Effective Blocking Time and Blocking Efficiency Under Different Blocking Parameters

We pressed the rat's Achilles tendon with a pressure gauge, and kept the pressure at 1∼2 N, and each press lasted 3 seconds. While pressing the Achilles tendon, a blocking signal was applied to the sciatic nerve through the blocking electrode. As shown in Fig. 3, when the blocking signal is applied to the sciatic nerve, the induced spastic EMG signal disappears, but when the blocking signal amplitude is reduced

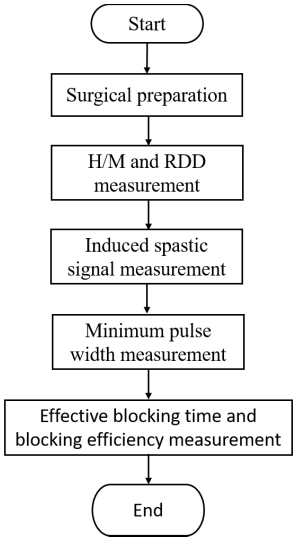

Fig. 4. Experimental flowchart.

to a certain extent, the spastic EMG signal begins to appear. The effective blocking time is the time during which the nerve signal conduction can be completely blocked when the blocking signal is applied. The effective blocking time is defined as the time from the disappearance of the spastic EMG signal to its reappearance. Its reappearance means that the EMG amplitude is higher than the resting EMG RMS value of 0.08 V.

The variable E_b is defined as the blocking efficiency, V_{bb} is defined as the RMS value of the EMG signal before blocking, V_{ab} is defined as the RMS value of the EMG signal after blocking.

$$E_b = \frac{(V_{bb} - V_{ab})}{V_{bb}} \tag{1}$$

As shown in Eq. 1, the ratio of the change in the RMS value of the spastic EMG signal to the RMS value of the spastic EMG signal before blocking was defined as the blocking efficiency. 10 blocking signals were continuously output in each experiment, and the blocking signal amplitude was set as 3∼6 V (step 0.5 V) in turn and the signal pulse width was set as the minimum pulse width under the corresponding amplitude. When these signals are applied, the single pulse width is adjusted to 300 ms and applied again. Waveforms with different blocking parameters were applied to the nerves and the gastrocnemius EMG signal was recorded multiple times, and the average value of the results was taken as the blocking result of a certain parameter blocking waveform in a single rat.

G. The Overall Process of the Experiment

In this paper, the experiment was carried out on 8 normal rats and 8 T9 spinal cord transection rats. The normal rats were used for measurement experiment of the H/M-ratio and the RDD, and T9 spinal cord transection rats were subjected to all of the experiments.

The entire experimental process is shown in Fig. 4. Each experimental animal had their H/M-ratio and RDD measured

after completion of the operation and the instrument connection. After completing the measurement of the H/M-ratio and the RDD, an appropriate amount of saline was injected into the wound, soaked the sciatic nerve, and the rat was allowed to rest for 5∼7 minutes. Then, absorbent paper was used to remove the saline in the wound, the gastrocnemius EMG signal in the non-stimulated state and the spasm EMG signal induced by external stimulation were recorded, and the minimum pulse width corresponding to different blocking signal amplitudes was measured. After completing the measurement, saline was injected into the wound again and the rat was allowed to rest for 5∼7 minutes. Finally, the effective blocking time and blocking efficiency corresponding to the different blocking signal parameters were measured. All rats were going through the experiments of 3 hours and then were euthanized.

H. Data Processing

All of the EMG signals in this paper were recorded using the commercial software LabChart and the graphs were prepared with Matlab. All collected data were analyzed using commercial statistical software packages (SPSS, IBM, USA). We use the statistical charts of data to observe the trends of variables and analyze the differences between different sets of data. First, we checked the homogeneity of the normal distribution and variance. If the data followed a normal distribution and the variance between the groups was homogeneous, univariate analysis was used. If the variance between groups was not homogeneous, the nonparametric statistical Kruskal-Wallis test was used.

Most of the data are displayed using box plots, the black dots in the box plot indicate the value of a single rat. The white dots represent the average of all rats. The two horizontal lines above and below the box represent the standard deviation of all rats. The box represents the value range of 25%-75%, and the horizontal line in the middle of the box represents the median. Three stars indicate that the p value of the significant difference test is less than 0.001, two stars indicate that the p value is less than 0.01. The data shown in the paper is the mean ± standard deviation of 8 animals.

III. Results

A. The H/M Ratio and the RDD

After 4 weeks of T9 spinal cord transection, the spastic rat's H-reflex was analysed and compared with that of normal rats. As shown in Fig. 5, the H/M-ratio of 8 normal rats was 0.27±0.08, and the H/M-ratio of 8 spastic rats was 0.91±0.13. Statistical analysis shows that the H/M-ratio of spastic rats after 4 weeks of spinal cord transection was significantly higher than that of normal rats, and there was a significant difference between two groups of data ($p < 10^{-3}$).

The RDD measurement results for the spastic rats and normal rats are shown in Fig. 6. Based on the H-reflex value at the frequency of 0.1 Hz, the H-reflex values at other frequencies have been converted into percentages. When the frequency is 0.5 Hz, the H-reflex value of normal rats will drop sharply, and as the frequency increases, the H-reflex decreases slowly (except for 5 Hz). The H-reflex value of spastic rats gradually

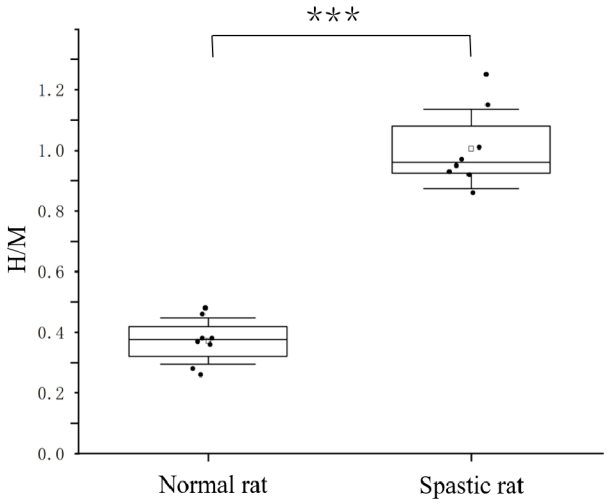

Fig. 5. H/M ratio of 8 spastic and 8 normal rats. The value was found to be normally distributed. A one-way analysis of variance revealed a significant difference between the H/M of normal rat and spastic rat ($p^{***} < 10^{-3}$).

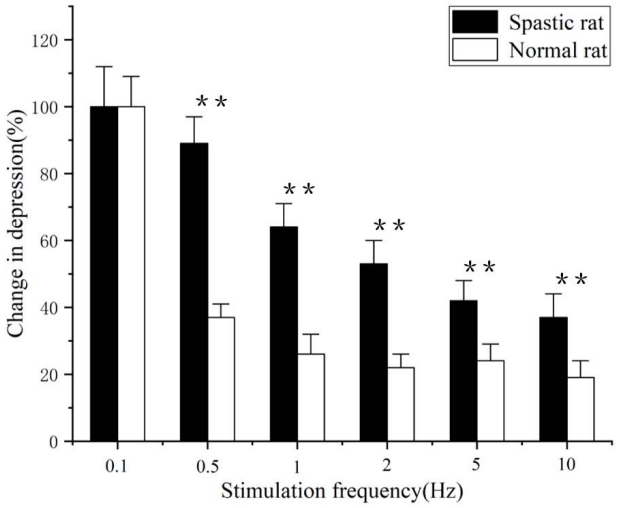

Fig. 6. The results of frequency-dependent inhibition in 8 spastic rats and 8 normal rats. The value was found to be normally distributed. A one-way analysis of variance revealed a significant difference between the two sets of data ($p^{**} < 10^{-2}$).

decreased with increasing frequency. Statistical analyses show that when the frequency is greater than 0.1 Hz, the change in RDD of the spastic rats was significantly smaller than that of normal rats, and there was a significant difference between the two sets of data($p^{**} < 0.01$).

B. Induction of the Spastic EMG Signal of Gastrocnemius in Rats With T9 Spinal Cord Transection

Four weeks after T9 spinal cord transection, the gastrocnemius EMG signal of the spastic rats was recorded for 2 minutes in the awake state. The 26-second time-domain diagram is shown in the upper part of Fig. 7. The spastic EMG signal burst occasionally had a maximum amplitude of 1.2 V. The longest duration was 870 ms. The maximum interval between

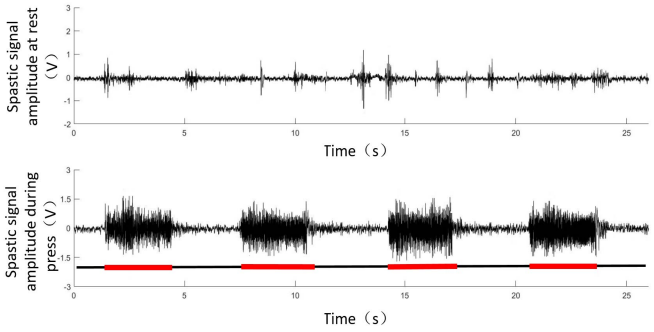

Fig. 7. Time-domain diagram of the spastic EMG signals recorded on the rat's gastrocnemius muscle at rest and when the Achilles tendon was pressed. The red line indicates that the rat's Achilles tendon was pressed during this time.

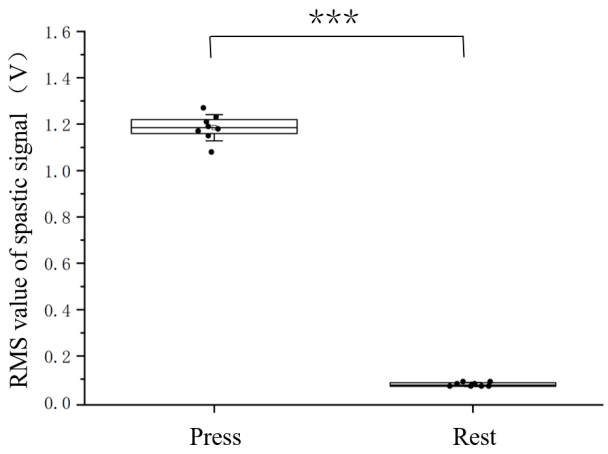

Fig. 8. The RMS value of the EMG signal of 8 rats with spasms at rest and when pressing the Achilles tendon. The value was found to be normally distributed. One-way analysis of variance showed that there is a significant difference in the RMS value in the two cases. ($p^{***} < 10^{-3}$).

signal clusters was 39 s, and the minimum was 140 ms. When pressing on the rat's Achilles tendon, the amplitude of the gastrocnemius spastic EMG signal increased significantly, and during the period of pressing on the Achilles tendon, the spastic EMG signal amplitude remained at a relatively stable value and immediately decreased to the level before pressing after the compression was stopped. We randomly took the EMG signal at rest for 3 s to calculate its RMS value and compared it with the RMS value of the EMG signal during the 3-s pressing period. The result is shown in Fig. 8. The EMG signal RMS value during pressing was significantly higher than that at rest. The RMS value of the EMG signal during pressing was 1.18±0.06, and the RMS value of the EMG signal at rest was 0.08±0.01. The results of the difference analysis showed that there was a significant difference between two sets of data ($p < 10^{-3}$).

C. The Minimum Pulse Width Under Different Blocking Amplitudes

As shown in Fig. 9, When the stimulation signal is applied alone, the gastrocnemius muscle bursts with an EMG signal. When the blocking signal with appropriate parameters is

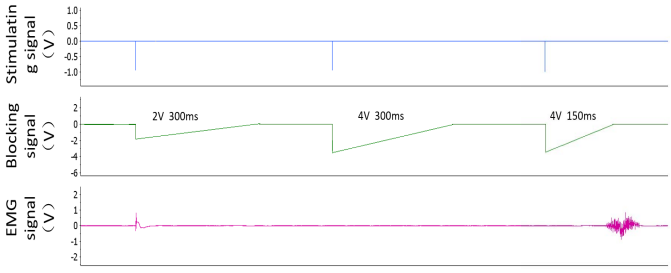

Fig. 9. Blocking results under different conditions.

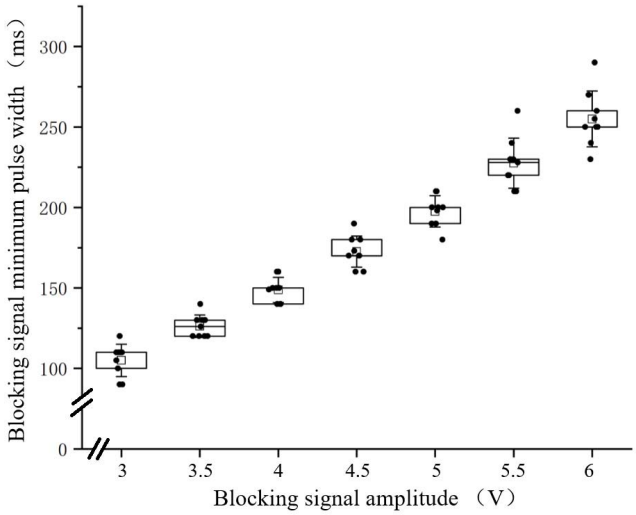

Fig. 10. Minimum pulse width under different blocking amplitudes (in 8 spastic rats).

applied alone, the gastrocnemius muscle does not contract and no EMG signal is generated. Then, we applied the stimulus signal and the blocking signal at the same time, the conduction of the nerve signals cannot be blocked, when the amplitude of the blocking signal was too low. The nerve was excited at the moment of stopping blocking signal, when the pulse width of the blocking signal was too small.

Applying blocking signals of different amplitudes to the sciatic nerve, the corresponding minimum pulse width of the blocking signal is shown in Fig. 10. As the blocking signal amplitude increases from 3 V to 6 V, the minimum pulse width of the blocking signal gradually increases (3∼6 V: 105±10.7, 126±7.44, 149±8.35, 173±10.4, 198±10.4, 228±16.7, 255±18.5).

D. Effective Blocking Time Under Different Blocking Amplitudes

As shown in Fig. 11, when the blocking signal pulse width is fixed at 300 ms, as the blocking signal amplitude increases, the effective blocking time also increases. The minimum effective blocking time is 55 ms, and the maximum is 164 ms. The overall range of change is 66.3±5.09 ∼ 156±6 ms.

The gastrocnemius spasm signal detected after 10 consecutive applications of blocking signals is shown in Fig. 12. As the amplitude of the blocking signal increases, the

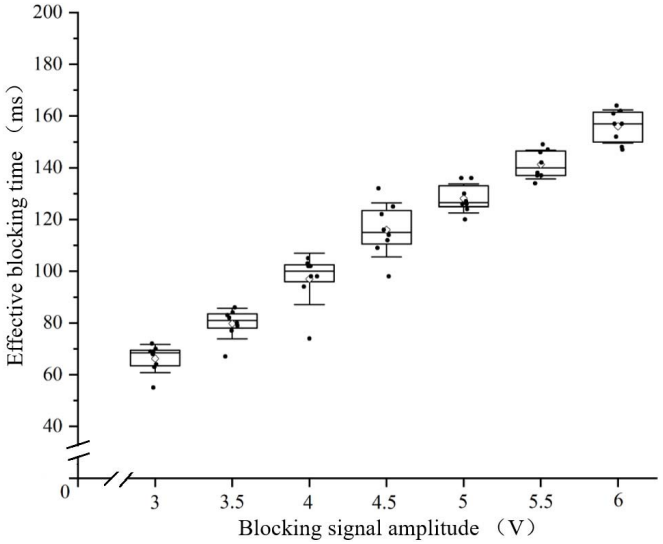

Fig. 11. Effective blocking time under the condition of different blocking amplitudes with a 300 ms pulse width (in 8 spastic rats).

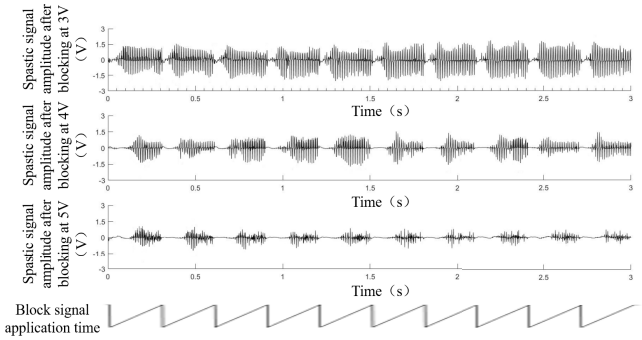

Fig. 12. Blocking effect under different blocking amplitudes with a 300 ms pulse width.

time during which the spastic signal is completely blocked increases, and the overall amplitude of the spastic signal decreases. When 10 blocking signals with a minimum pulse width are continuously applied, as the amplitude of the blocking signal increases, the effective blocking time also increases, and the overall range of change is 30.0±2.99∼128±9.9 ms (Fig. 13). Under the same blocking signal amplitude, the effective blocking time between the minimum pulse width and 300 ms fixed pulse width was compared. The results are shown in Fig. 14. Under all tested amplitudes, the effective blocking time at a fixed pulse width of 300 ms is greater than the value at the minimum pulse width. The test results showed that there are significant differences between the two sets of data under different blocking amplitudes ($p < 10^{-3}$).

E. Blocking Efficiency Under Different Blocking Signal Amplitudes at a 300-ms Pulse Width

When a continuous blocking signal with a fixed pulse width of 300 ms and different blocking amplitudes was applied to the sciatic nerve of the spastic rats, the RMS change value of the gastrocnemius spasm signal detected after the blocking signal was applied is divided by the RMS value before the blocking signal was applied. The blocking efficiency obtained is shown in Fig. 15. When the blocking signal amplitude changes

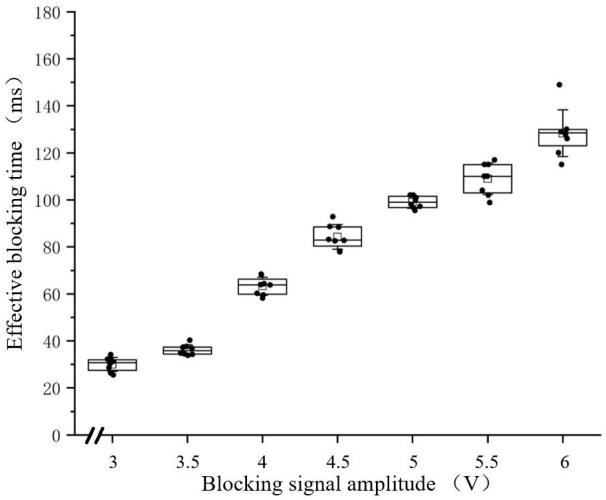

Fig. 13. Effective blocking time under different blocking amplitudes and their corresponding minimum pulse widths (in 8 spastic rats).

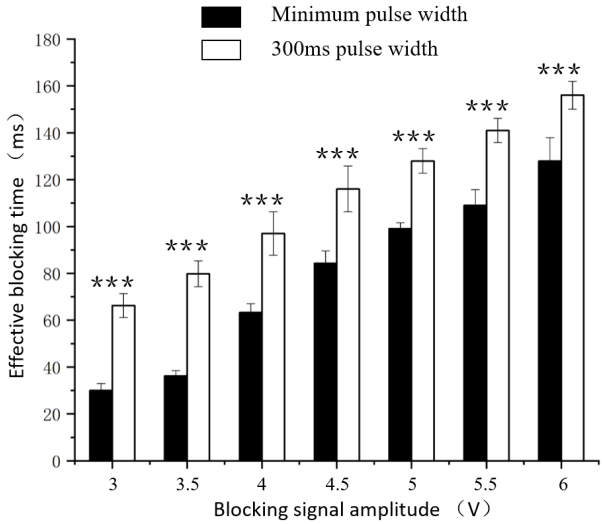

Fig. 14. Comparison of effective blocking time between minimum blocking pulse width and 300 ms fixed pulse width. The value was found to be normally distributed. A one-way analysis of variance revealed a significant difference between the two sets of data ($p^{***} < 10^{-3}$).

from 3 V to 6 V, the blocking efficiency continues to increase by 0.03±0.02, 0.14±0.03, 0.29±0.05, 0.44±0.03, 0.63±0.04, 0.69±0.03, and 0.72±0.04, respectively. The change in blocking efficiency first slowly increases, and then increases rapidly during the period of 4∼5 V. When the amplitude is greater than 5 V, the increasing speed of blocking efficiency becomes slower.

IV. Discussion

In the past few decades, a variety of spastic animal models have been developed and used to answer questions about the pathophysiology of muscle spasm and explore new therapies to inhibit muscle spasm [34]. In this paper, the T9 spinal cord segments of rats were completely transected. After a rat had undergone the spinal cord transection, its lower limbs were completely paralyzed, and the muscles were in a relaxed state after waking up. When the rats were carefully cared for and survived for 4 weeks, their lower limbs developed convulsions

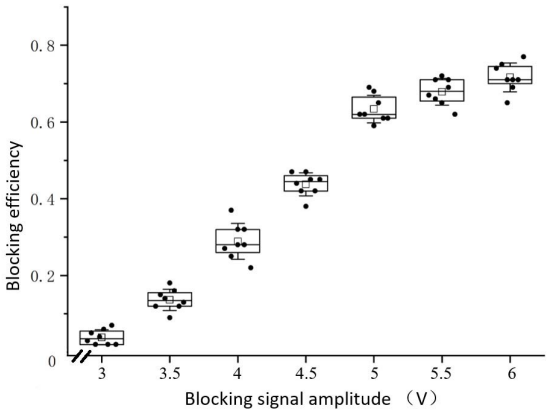

Fig. 15. Blocking efficiency under different blocking signal amplitudes at a 300-ms pulse width (in 8 spastic rats).

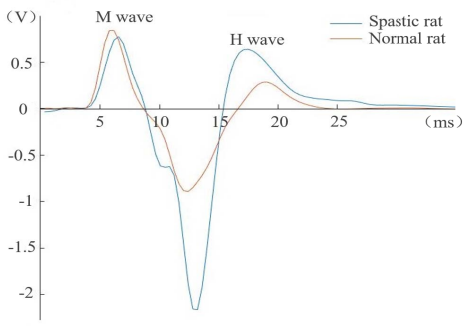

Fig. 16. The H-reflex EMG signal of spastic and normal rats.

and occasionally intermittent tremors. When the spinal cord is transected, the main mechanisms that cause lower limb spasms are as follows:

1) After spinal cord motor neurons lose the inhibitory effect of the upper neuron, the spinal cord activity increases, especially the excitability of γ motor neurons in the anterior horn of the spinal cord. The nerve impulse sent by the γ motor neuron can increase the sensitivity of the muscle spindle so that the muscle spindle receptor is in a sensitive state. Through sensory afferent nerve fibers, the excitability of spinal α motor neurons increases, and muscle contraction activity is strengthened [35]–[37].

2) Spinal cord injury can cause significant activation of glial cells, and local excitatory neurons are activated through the release of secondary excitatory amino acids [38]–[41].

Usually, researchers reflect the increase in motor neuron excitability through the changes of H/M ratio and RDD [4], [14]. As shown in Fig. 16, due to the loss of the inhibition of the upper neuron, the H-reflex is enhanced. The H-wave amplitude increases and the M-wave amplitude does not change, so the H/M-ratio increases.

As shown in Fig. 5, 4 weeks after spinal cord transection, the H-reflex of spastic rats was enhanced, and the H/M-ratio increased and was significantly higher than that in normal rats. As shown in Fig. 6, with the increase in the stimulation frequency, the H-reflex amplitude of normal rats was obviously suppressed, but the H-reflex amplitude of spastic rats was not as obvious as that of normal rats, and the RDD was weakened. Other studies on rats and humans have shown that after spinal cord injury, the H-reflex is significantly enhanced, and the RDD is also weakened, what is also consistent with our experimental results [12], [34], [37]. Jose *et al.* also quantified the number of interneurons in the lamina of rats with 3 months after spinal cord transection, and there was no obvious loss. Based on that, they deduced that the lower limb spasm and super-reflex phenomena in the spinal cord transection model were mainly caused by the loss of downward tonic suppression [12].

In addition to quantifying the hyperactivity of the H-reflex, we also recorded the gastrocnemius muscle EMG signal of the spastic rat in the resting state for a long time. As shown in Fig. 7, in the resting state, the gastrocnemius muscles of spastic rats burst EMG signals intermittently, but the duration was short, and the interval between the EMG signal clusters was relatively long. When an external force is applied to the Achilles tendon of its lower limbs, the target muscle will burst a higher amplitude EMG signal within the duration of the force. Comparing the RMS value of the EMG signal at rest with the RMS value of the EMG signal when subjected to external force, the results show that the value during pressing is much higher than the value at rest (Fig. 8). These observations are similar to spasticity induced by spinal injuries in other rodents. When pressure was applied to the soles of spastic rats, an overactive myoelectric response is clearly recorded [12]. The main reason for this phenomenon is the lack of upper motor neuron suppression and the lower response threshold of spinal cord neurons to external stimuli.

In a previous study, we conducted a nerve signal blocking experiment on a bullfrog isolated sciatic nerve gastrocnemius muscle specimen. The electrode was used an asymmetric conformation, and the width of the electrode anode was larger than the width of the cathode. The experimental results showed that the blocking threshold is the smallest [33] when the anode width is 5 mm. In this paper, a 5 mm wide electrode anode was used. When the blocking signal is applied, the cell membrane under the anode is hyperpolarized, and the cell membrane under the cathode is depolarized. The width of the electrode anode is much larger than that of the cathode, the width of the hyperpolarized area of the cell membrane under the electrode anode is greater than the width of the depolarized area, so that the action potential generated during the depolarization process under the electrode cathode cannot be conducted out of the area under the whole electrode. When the nerve signal is conducted below the anode, the action potential reached is not enough to depolarize it because the cell membrane is in a hyperpolarized state, so the conduction of the action potential is blocked [42]. With the asymmetric electrode configuration, the spike trapping block can instantly block nerve signal conduction without causing nerve excitement. As shown in Fig. 10, as the amplitude of the blocking signal increases, the minimum pulse width of the blocking signal also linearly increases. When the voltage signal applied to the nerve is suddenly turned off, the nerve will be excited due to the stimulating effect of the anode off. To avoid this phenomenon, it is necessary to slow down the rate of voltage drop as much as possible. When the voltage of the blocking

signal increases, since the voltage drop rate cannot be changed, the minimum pulse width of the blocking signal will increase.

On the premise of preparing a stable spastic rat model, we tried to use nerve signal blocking technology based on the trapping principle to block the conduction of spastic nerve signals. When a single blocking signal is applied to a nerve, the spastic EMG signal first disappears completely within a period of time. When the amplitude of the blocking signal decreases to a certain value, the spastic EMG signal reappears, and as the blocking signal amplitude continues to decrease, the spastic EMG signal amplitude will increase. As shown in Fig. 11, when the blocking pulse width is fixed at 300 ms, as the blocking signal amplitude increases, the effective blocking time also linearly increases. As shown in Fig. 13, when the minimum pulse width is used, the effective blocking time also increase as the amplitude of the blocking signal increases. However, comparing the effective blocking time under the same blocking signal amplitude with different blocking signal pulse widths, the effective time at a pulse width of 300 ms is significantly greater than the value at the minimum pulse width. This result indicates that it is not appropriate to use the minimum pulse width, and the appropriate blocking signal pulse width should be selected to more fully block the transmission of spastic nerve signals. The higher the amplitude of the blocking signal is, the longer the effective blocking time. However, an excessively high blocking signal amplitude will have an impact on the safety of nerve block, so a suitable blocking signal amplitude should be selected when the blocking requirement is met.

Although the spasm signal reappears after the effective blocking time, its amplitude is still significantly smaller than the value before the block, so the effective blocking time does not fully reflect the blocking effect. To better illustrate the effect of block, we divided the change in the RMS value of the spastic EMG signal after block by the RMS value of the spastic EMG signal before block to obtain the blocking efficiency under different amplitudes with a fixed pulse width of 300 ms. As shown in Fig. 15, the blocking efficiency also gradually increases as the amplitude of the blocking signal increases, when the pulse width of the blocking signal is fixed at 300 ms. The rate changes from fast to slow again. When the blocking signal is 5 V, the blocking efficiency is 63%.

Although nerve signal blocking technology based on the trapping principle cannot completely block the conduction of spastic nerve signals, it can instantly and reversibly block a part of the spastic nerve signal transmission without side effects. For the first time, we have successfully used nerve signal blocking technology to inhibit muscle spasms in an animal model of spasms, providing the feasibility of inhibiting muscle spasm by blocking nerve signals in the future.

As shown in our previous studies, there is no significant change in nerve conductivity after short-term block experiments, which shows that a short-term application of an inverted triangle block waveform will not cause nerve damage [33]. However, this paper used a single-phase inverted triangle blocking waveform. Only when a certain voltage value is reached, a blocking effect can be obtained. We can form a right-angled trapezoid by adding a plateau period, which can improve the blocking efficiency and appropriately reduce the peak value of the blocking signal. The safety of the waveform is dependent on the total charge of each cycle. That is calculated as the area of the waveform [26], [29]. When inputting the same amount of charge, the right-angled trapezoid waveform can reduce the blocking signal amplitude, extend the blocking signal time, and improve the blocking efficiency. If it acts on the nerve for a long time, it will inevitably cause nerve damage and electrode dissolution. Therefore, the waveform is not suitable for long-term use alone.

Ultimately, we need to solve the clinical problems. There are still many problems that need to be solved in STNB from the animal experiment stage to the clinical experiment stage. The first is the charge injection and safety issues. In the next research, we will study the biphasic charge balance inverted triangle blocking waveform. If the biphasic blocking waveform can also block the nerve signal conduction instantly and efficiently without exciting the nerve, then the STNB can block the nerve signal conduction for a long time. We also will combine spike trapping blocking technology with HF blocking technology to give full play to the advantages of both. The advantages of STNB is rapid, reversible and without an initial effect and the HF blocking can cause a long duration and complete blocking. In addition to these, we also can study the higher capacitive electrode material to extend the acceptable charge [43], [44]. Then, there is the problem of identifying and blocking pathological signals. All the nerve signals conducted on the sciatic nerve are blocked in this paper. There are not only abnormal spastic nerve signals, but also normal sensory and motor nerve signals. As a result, not only the gastrocnemius muscle spasm was suppressed, but also other muscles innervated if the sciatic nerve lose the control due to the block of nerve signals. This paper just proves that blocking the sciatic nerve signal can inhibit muscle spasm in the lower limbs, but it is obviously inappropriate to block all nerve signal transmission, which will affect the normal control and sensation of the limbs. In the future, we will study how to recognize spasticity signals and block them individually. The ultimate goal of the research is to find a new clinically applicable method that can inhibit muscle spasm without affecting the normal activities of the limbs.

V. Conclusion

We prepared a rat model of spasm and inhibited the muscle spasms by blocking the conduction of pathological nerve signals. By transecting the T9 spinal cords of rats and quantifying the changes in the H/M-ratio and RDD, and the muscle spastic EMG signal after modelling, the reliability of the rat spasticity model was demonstrated. After applying different parameters of blocking signals to the sciatic nerve of the spastic rats, it was found that as the amplitude of the blocking signal increased, the effective blocking time and the blocking efficiency for spasticity inhibition increased. Though the highest blocking efficiency in all experiments was 73%, which could not completely inhibit the muscle spasms, the feasibility of inhibiting the muscle spasticity by blocking the pathological nerve signal has been verified.

REFERENCES

[1] J. R. H. Foran, S. Steinman, I. Barash, H. G. Chambers, and R. L. Lieber, "Structural and mechanical alterations in spastic skeletal muscle," *Develop. Med. Child Neurol.*, vol. 47, no. 10, pp. 713–717, 2010.

[2] C. Sköld, R. Levi, and Å. Seiger, "Spasticity after traumatic spinal cord injury: Nature, severity, and location," *Arch. Phys. Med. Rehabil.*, vol. 80, no. 12, pp. 1548–1557, 1999.

[3] S. Kirshblum, "Treatment alternatives for spinal cord injury related spasticity," *J. Spinal Cord Med.*, vol. 22, no. 3, pp. 199–217, Jan. 1999.

[4] H. Hultborn, "Changes in neuronal properties and spinal reflexes during development of spasticity following spinal cord lesions and stroke: Studies in animal models and patients," *J. Rehabil. Med.*, vol. 35, pp. 46–55, Oct. 2003.

[5] D. J. Bennett, L. Sanelli, C. L. Cooke, P. J. Harvey, and M. A. Gorassini, "Spastic long-lasting reflexes in the awake rat after sacral spinal cord injury," *J. Neurophysiol.*, vol. 91, no. 5, pp. 2247–2258, 2004.

[6] V. Dietz and T. Sinkjaer, "Spastic movement disorder: Impaired reflex function and altered muscle mechanics," *Lancet Neurol.*, vol. 6, no. 8, pp. 725–733, 2007.

[7] R. T. Katz, G. P. Rovai, C. Brait, and W. Z. Rymer, "Objective quantification of spastic hypertonia: Correlation with clinical findings," *Arch. Phys. Med. Rehabil.*, vol. 73, no. 4, pp. 339–347, Apr. 1992.

[8] D. J. Bennett, M. Gorassini, K. Fouad, L. Sanelli, Y. Han, and J. Cheng, "Spasticity in rats with sacral spinal cord injury," *J. Neurotrauma*, vol. 16, no. 1, pp. 69–84, Jan. 1999.

[9] G. K. Kanellopoulos, H. Kato, C. Y. Hsu, and N. T. Kouchoukos, "Spinal cord ischemic injury: Development of a new model in the rat," *Stroke*, vol. 28, no. 12, p. 2532, 1997.

[10] G. Z. Sufianova, L. A. Usov, A. A. Sufianov, A. G. Shapkin, and L. Y. Raevskaya, "New minimally invasive model of spinal cord ischemia in rats," *Bull. Exp. Biol. Med.*, vol. 133, no. 1, pp. 98–101, 2002.

[11] Y. Yu *et al.*, "Protective effect of local intraspinal perfusion with Danshen injection on acute spinal cord injury," (in Chinese), *J. Chin. Exp. Surg.*, vol. 21, no. 8, pp. 993–994, 2004.

[12] J. A. Corleto *et al.*, "Thoracic 9 spinal transection-induced model of muscle spasticity in the rat: A systematic electrophysiological and histopathological characterization," *PLoS ONE*, vol. 10, no. 12, Dec. 2015, Art. no. e0144642.

[13] G.-X. Shi, C.-Y. Yang, M.-M. Wu, L.-P. Guan, L.-P. Wang, and C.-Z. Liu, "Muscle hypertonia after permanent focal cerebral ischemia in rats: A qualitative and quantitative behavioral and electrophysiological study," *Int. J. Neurosci.*, vol. 123, no. 8, pp. 575–581, Aug. 2013.

[14] S. Lee, T. Toda, H. Kiyama, and T. Yamashita, "Weakened rate-dependent depression of Hoffmann's reflex and increased motoneuron hyperactivity after motor cortical infarction in mice," *Cell Death Disease*, vol. 5, no. 1, p. e1007, Jan. 2014.

[15] J. Lui, M. Sarai, and P. B. Mills, "Chemodenervation for treatment of limb spasticity following spinal cord injury: A systematic review," *Spinal Cord*, vol. 53, no. 4, pp. 252–264, Apr. 2015.

[16] C. Michael *et al.*, "Effect of intrathecal baclofen on pain and quality of life in poststroke spasticity: A randomized trial (SISTERS)," *Stroke*, vol. 49, no. 9, pp. 2129–2137, 2018.

[17] B. Amatya, F. Khan, D. Bensmail, and A. Yelnik, "Non-pharmacological interventions for spasticity in adults: An overview of systematic reviews," *Ann. Phys. Rehabil. Med.*, vol. 61, p. e268, Jul. 2018.

[18] O. M. Katalinic, L. A. Harvey, R. D. Herbert, A. M. Moseley, N. A. Lannin, and K. Schurr, *Stretch for the Treatment and Prevention of Contractures*. Hoboken, NJ, USA: Wiley, 2010.

[19] N. A. Lannin and L. Ada, "Neurorehabilitation splinting: Theory and principles of clinical use," *NeuroRehabilitation*, vol. 28, no. 1, pp. 21–28, 2011.

[20] Y. A. Patel and R. J. Butera, "Challenges associated with nerve conduction block using kilohertz electrical stimulation," *J. Neural Eng.*, vol. 15, no. 3, Jun. 2018, Art. no. 031002.

[21] K. L. Kilgore and N. Bhadra, "Reversible nerve conduction block using kilohertz frequency alternating current," *Neuromodulation, Technol. Neural Interface*, vol. 17, no. 3, pp. 242–255, Aug. 2013.

[22] D. M. Ackermann, Jr., E. L. Foldes, N. Bhadra, and K. L. Kilgore, "Effect of bipolar cuff electrode design on block thresholds in high-frequency electrical neural conduction block," *IEEE Trans. Neural Syst. Rehabil. Eng.*, vol. 17, no. 5, pp. 469–477, Oct. 2009.

[23] Y. A. Patel, B. S. Kim, and R. J. Butera, "Kilohertz electrical stimulation nerve conduction block: Effects of electrode material," *IEEE Trans. Neural Syst. Rehabil. Eng.*, vol. 26, no. 1, pp. 11–17, Jan. 2018.

[24] X. Zhang, J. R. Roppolo, W. C. de Groat, and C. Tai, "Mechanism of nerve conduction block induced by high-frequency biphasic electrical currents," *IEEE Trans. Biomed. Eng.*, vol. 53, no. 12, pp. 2445–2454, Dec. 2006.

[25] J. A. Tanner, "Reversible blocking of nerve conduction by alternating-current excitation," *Nature*, vol. 195, no. 4842, pp. 712–713, 1962.

[26] D. M. Ackermann, Jr., N. Bhadra, E. L. Foldes, X. F. Wang, and K. L. Kilgore, "Effect of nerve cuff electrode geometry on onset response firing in high-frequency nerve conduction block," *IEEE Trans. Neural Syst. Rehabil. Eng.*, vol. 18, no. 6, pp. 658–665, Dec. 2010.

[27] M. Franke, T. Vrabec, J. Wainright, N. Bhadra, N. Bhadra, and K. Kilgore, "Combined KHFAC + DC nerve block without onset or reduced nerve conductivity after block," *J. Neural Eng.*, vol. 11, no. 5, Oct. 2014, Art. no. 056012.

[28] D. M. Ackermann, Jr., N. Bhadra, E. L. Foldes, and K. L. Kilgore, "Conduction block of whole nerve without onset firing using combined high frequency and direct current," *Med. Biol. Eng. Comput.*, vol. 49, no. 2, pp. 241–251, Feb. 2011.

[29] J. D. Miles, K. L. Kilgore, N. Bhadra, and E. Lahowetz, "Effects of ramped amplitude waveforms on the onset response of high-frequency mammalian nerve block," *J. Neural Eng.*, vol. 4, no. 4, pp. 390–398, 2007.

[30] M. Gerges, E. L. Foldes, D. M. Ackermann, N. Bhadra, N. Bhadra, and K. L. Kilgore, "Frequency- and amplitude-transitioned waveforms mitigate the onset response in high-frequency nerve block," *J. Neural Eng.*, vol. 7, no. 6, Dec. 2010, Art. no. 066003.

[31] D. M. Ackermann, Jr., E. L. Foldes, N. Bhadra, and K. L. Kilgore, "Nerve conduction block using combined thermoelectric cooling and high frequency electrical stimulation," *J. Neurosci. Methods*, vol. 193, no. 1, pp. 72–76, Oct. 2010.

[32] Z.-G. Wang, X.-Y. Lu, Y.-J. Gao, J.-J. Zhang, and B. Wang, "Experimental study on nerve signals block for spasticity based on antimissile strategy," in *Proc. 40th Annu. Int. Conf. IEEE Eng. Med. Biol. Soc. (EMBC)*, Jul. 2018, pp. 2260–2263.

[33] J. Zhang, Y. Feng, X.-Y. Lu, and Z. Wang, "Neural signal blocking based on spike trapping principle: Effect of electrode and pulse parameters," *IEEE Access*, vol. 8, pp. 64545–64554, 2020.

[34] X. Wu and R. Jin, "Evaluation method of rodent spasticity model," (in Chinese), *Theory Pract. Rehabil. China*, vol. 25, no. 6, pp. 648–651, 2019.

[35] C. Yates, K. Garrison, N. B. Reese, A. Charlesworth, and E. Garciarill, *Chapter 11–Novel Mechanism for Hyperreflexia and Spasticity*. Amsterdam, The Netherlands: Elsevier, 2011.

[36] S. Schindler-Ivens and R. K. Shields, "Low frequency depression of H-reflexes in humans with acute and chronic spinal-cord injury," *Exp. Brain Res.*, vol. 133, no. 2, pp. 233–241, Jul. 2000.

[37] S. Kapitza *et al.*, "Tail spasms in rat spinal cord injury: Changes in interneuronal connectivity," *Exp. Neurol.*, vol. 236, no. 1, pp. 179–189, Jul. 2012.

[38] O. Kakinohana *et al.*, "Development of GABA-sensitive spasticity and rigidity in rats after transient spinal cord ischemia: A qualitative and quantitative electrophysiological and histopathological study," *Neuroscience*, vol. 141, no. 3, pp. 1569–1583, Jan. 2006.

[39] A. V. Muralt, *Die Grundlagen der Entwicklung der Neurophysiologie*. Berlin, Germany: Springer, 1958.

[40] T. Fellin, O. Pascual, S. Gobbo, T. Pozzan, P. G. Haydon, and G. Carmignoto, "Neuronal synchrony mediated by astrocytic glutamate through activation of extrasynaptic NMDA receptors," *Neuron*, vol. 45, no. 1, p. 177, Jan. 2005.

[41] Yang and L., "A novel Ca^{2+}-independent signaling pathway to extracellular signal-regulated protein kinase by coactivation of NMDA receptors and metabotropic glutamate receptor 5 in neurons," *J. Neurosci. Off. J. Soc. Neurosci.*, vol. 24, no. 48, pp. 10846–10857, 2004.

[42] N. Accornero, G. Bini, G. L. Lenzi, and M. Manfredi, "Selective Activation of peripheral nerve fibre groups of different diameter by triangular shaped stimulus pulses," *J. Physiol.*, vol. 273, no. 3, pp. 539–560, 1977.

[43] T. Vrabec, N. Bhadra, J. Wainright, N. Bhadra, M. Franke, and K. Kilgore, "Characterization of high capacitance electrodes for the application of direct current electrical nerve block," *Med. Biol. Eng. Comput.*, vol. 54, no. 1, pp. 191–203, Jan. 2016.

[44] A. Ghazavi and S. F. Cogan, "Electrochemical characterization of high frequency stimulation electrodes: Role of electrode material and stimulation parameters on electrode polarization," *J. Neural Eng.*, vol. 15, no. 3, Jun. 2018, Art. no. 036023.